SUPPORTING INFORMATION

From Linear Molecular Chains to Extended Polycyclic Networks: Polymerization of Dicyanoacetylene

Huiyang Gou,[*,†,‡,°] Li Zhu,[†,°], Haw-Tyng Huang,[¶,■] Arani Biswas,[§,■] Derek W. Keefer,[§,■] Brian L. Chaloux,[‖,♦] Clemens Prescher,[⊥] Liuxiang Yang,[†,‡] Duck Young Kim,[†,‡] Matthew D. Ward,[†] Jordan Lerach,[■] Shengnan Wang,[#] Artem R. Oganov,[#,▽] Albert Epshteyn,[‖] John V. Badding,[§,■,¶,□] Timothy A. Strobel[*,†]

[†]Geophysical Laboratory, Carnegie Institution of Washington, Washington, DC 20015, USA
[‡]Center for High Pressure Science and Technology Advanced Research, Beijing 100094, China.
[¶]Department of Materials Science and Engineering, The Pennsylvania State University, University Park, PA 16802, USA.
[■]Materials Research Institute, The Pennsylvania State University, University Park, PA 16802, USA.
[§]Department of Chemistry, The Pennsylvania State University, University Park, PA 16802, USA.
[‖]Naval Research Laboratory, 4555 Overlook Ave., SW, Washington, DC 20375, USA
[♦]NRC Postdoctoral Associate, Naval Research Laboratory, 4555 Overlook Ave., SW, Washington, DC 20375, USA
[⊥]Center for Advanced Radiation Sources, University of Chicago, Argonne, IL 60437, USA
[#]Department of Geosciences, Center for Materials by Design, and Institute for Advanced Computational Science, State University of New York, Stony Brook, NY 11794-2100
[▽]Skolkovo Institute of Science and Technology, Skolkovo Innovation Center, 3 Nobel St., Moscow 143026, Russia.
[□]Department of Physics, The Pennsylvania State University, University Park, PA 16802, USA.

[°]Contributed equally to this work
*(H.G.) E-mail: huiyang.gou@hpstar.ac.cn
*(T.A.S.) E-mail: tstrobel@ciw.edu

Analysis of Single-Crystal X-ray Diffraction of C_4N_2

The solution and refinement of C_4N_2 were straightforward when compared to the known structure.[1] However, with the limited number of reflections collected, it was not possible to obtain reasonable anisotropic displacement parameters and the presented refinement is isotropic.

The structure of C_4N_2 is shown in Figure S1. The C_4N_2 molecule is expected to be linear from previous spectroscopic and crystallographic determinations.[1-3] The current refinement finds that the molecule has bond angles of 169.41(2.57) and 172.07(1.98) degrees. This departure from the expected linear arrangement could be ascribed to several possible factors, including low data completeness, large angular errors, and/or high-pressure distortions. The bond distances for C_4N_2 are listed in Table S1 and may be compared with those reported for the previous low-temperature refinement.[1] The C≡C has a bond distance of 1.140(20) Å which is shorter than that for the low-temperature structure of 1.19 Å. The C≡N bond compares favorably with a distance of 1.138(11) Å compared to 1.14 Å and the C1−C2 bond is slightly elongated at 1.434(12) Å compared to 1.37 Å in the low-temperature structure.

Table S1. Crystallographic Details for C_4N_2 at 0.2 GPa

Crystal System	Monoclinic
Space Group	$P2_1/c$
a / Å	3.878(1)
b/ Å	6.058(1)
c / Å	9.026(2)
β / °	98.943(30)
V / Å^3	209.45(7)
Z	2
Density, ρ_{calc} (g/cm^3)	1.206
T /K	293 (2)
Absorption Coefficient (mm^{-1})	0.081
Reflections Collected	41
Data/Parameters/Restraints	30/13/0
Data Completeness	0.150
R_{int}	0.0079
R(F) [I > 2σ(I)][a]	0.0449
$R_w(F_o^2)$[b]	0.0943

[a]$R(F) = \sum||F_o|-|F_c||/\sum|F_o|$ for $F_o^2 > 2\sigma(F_o^2)$. [b]$R_w(F_o^2) = \{\sum[w(F_o^2 - F_c^2)^2] / \sum wF_o^4\}^{1/2}$ for all data. $w^{-1} = \sigma^2(F_o^2) + (0.0680F_o^2)^2$ for $F_o^2 \geq 0$; $w^{-1} = \sigma^2(F_o^2)$ for $F_o^2 < 0$.

Table S2. Selected Interatomic Distances and Angles for C_4N_2 at 0.01 GPa

Interaction	Distance (Å)	Interaction	Angle (°)
N1−C2	1.138(11)	C1−C1−C2	169.41 (2.57)
C1−C1	1.140(20)	N1−C2−C1	172.07(1.98)
C1−C2	1.434(12)		

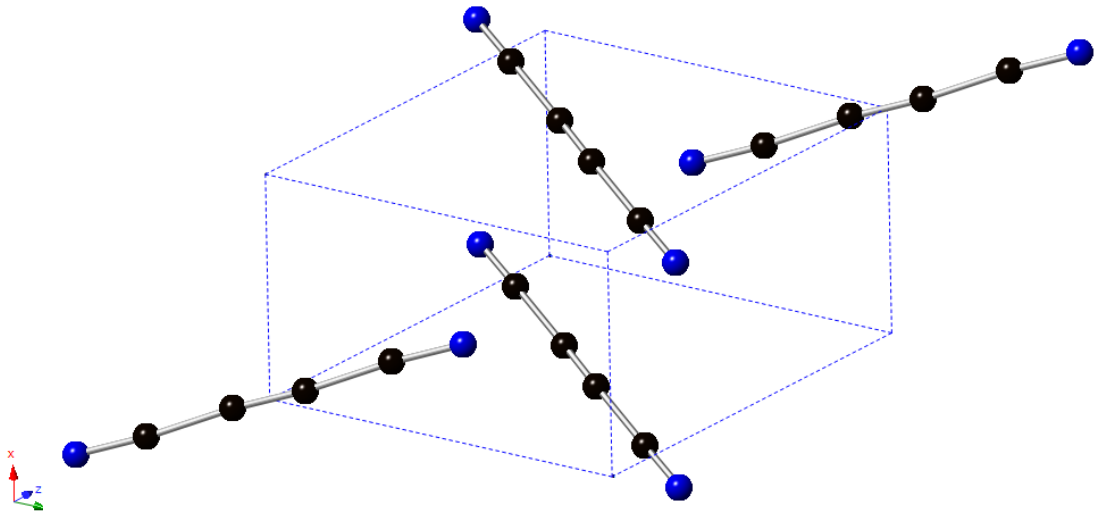

Figure S1. Unit cell of C_4N_2. Black and blue spheres indicate carbon and nitrogen, respectively.

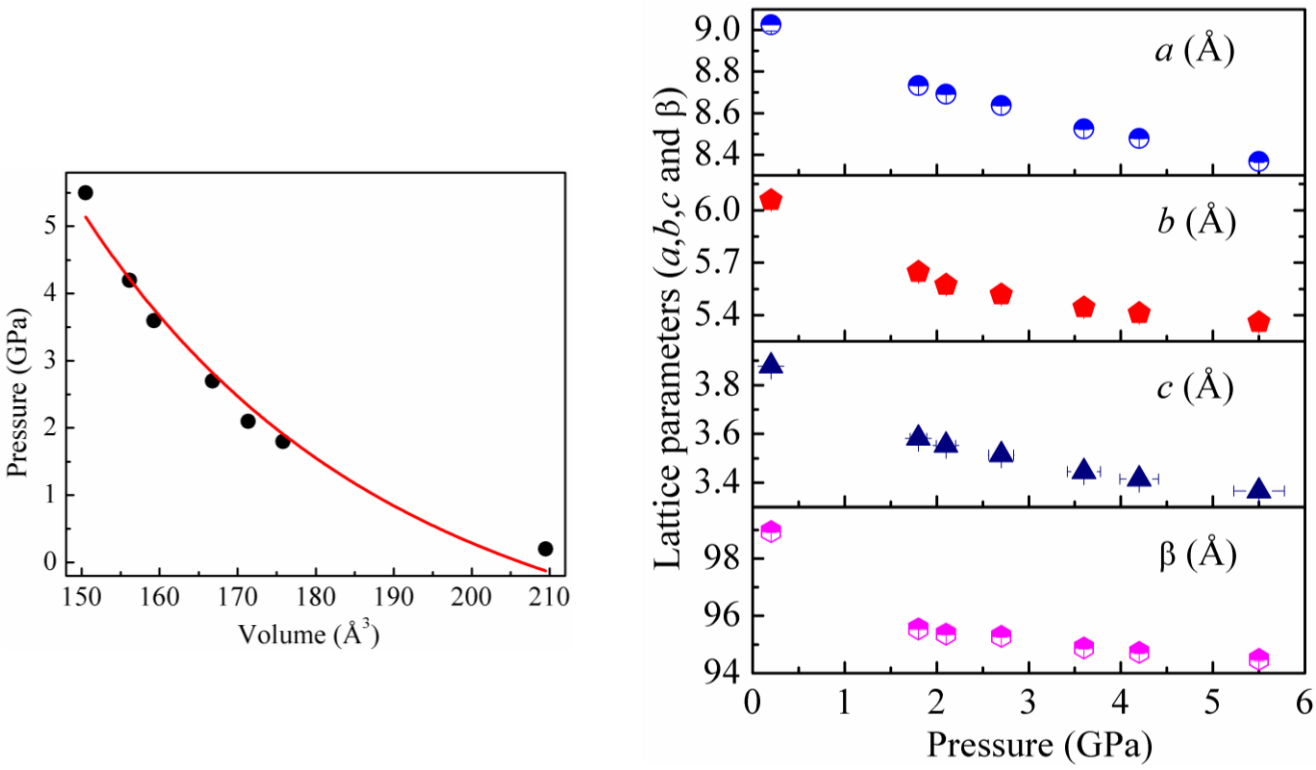

Figure S2. Pressure dependence of the volume and lattice parameters (*a*, *b*, *c* and *β*) as a function of pressure up to 5.5 GPa for C_4N_2. The bulk modulus of C_4N_2 is 8.60 ± 1.2 GPa, with B_0 = 4.0 (fixed) and V_0 = 206.4 Å^3 by fitting a second-order Birch-Murnaghan equation of state (red line).

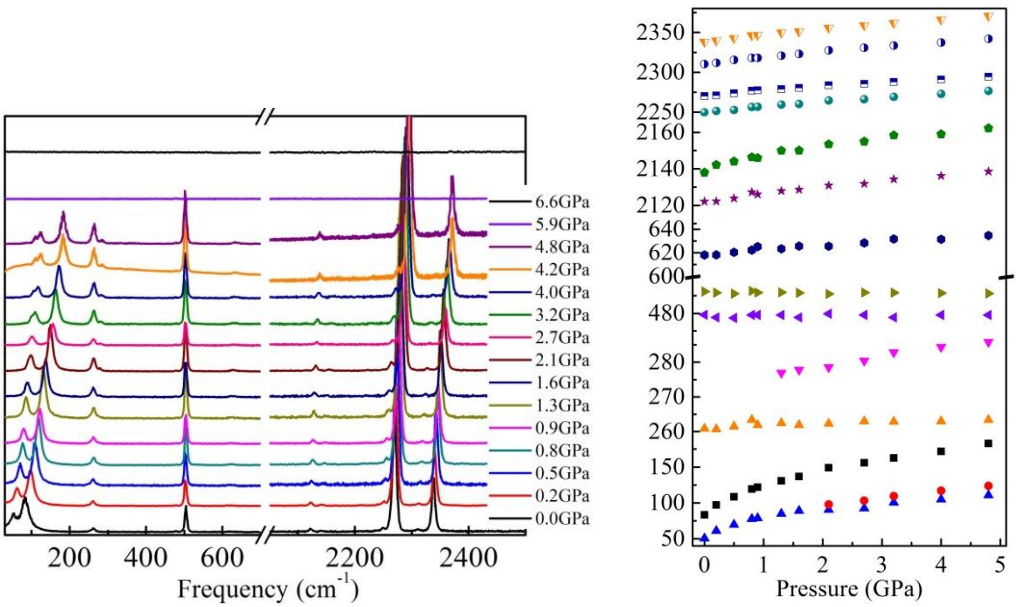

Figure S3. Pressure dependence of Raman spectra of C_4N_2 at room temperature (left) and the individual mode frequencies (right).

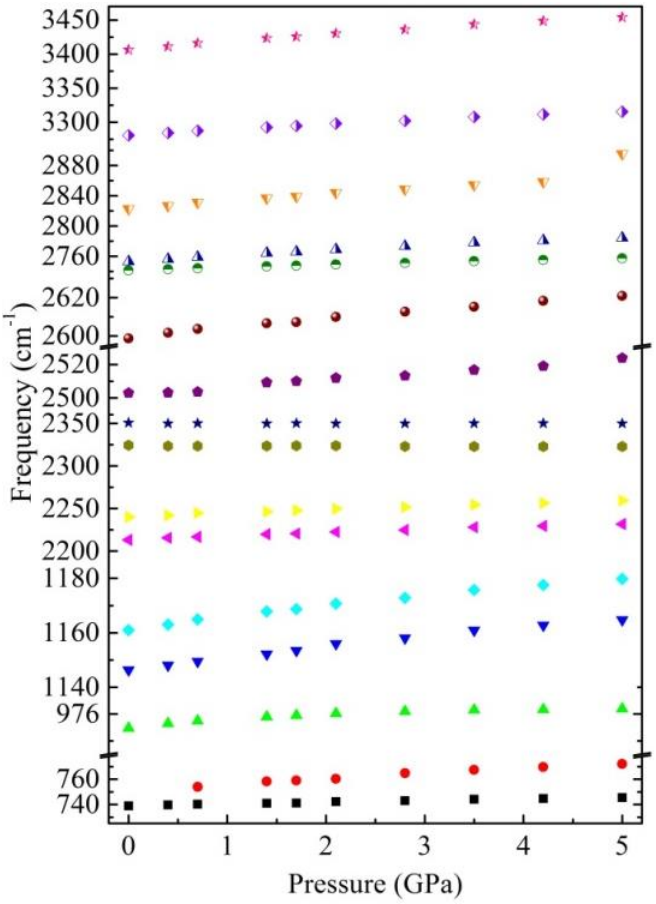

Figure S4. Pressure dependence of IR modes of C_4N_2 at room temperature.

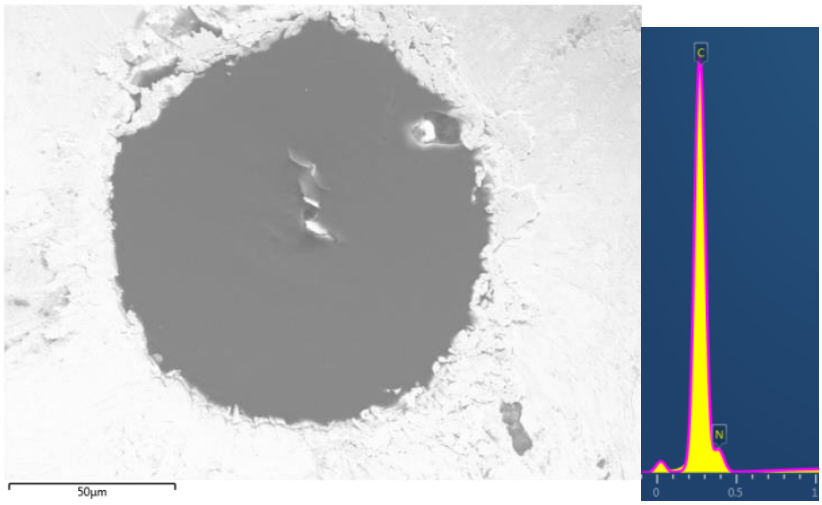

Figure S5. SEM image of recovered C_4N_2 sample within Re gasket (left) and representative EDS spectrum (right).

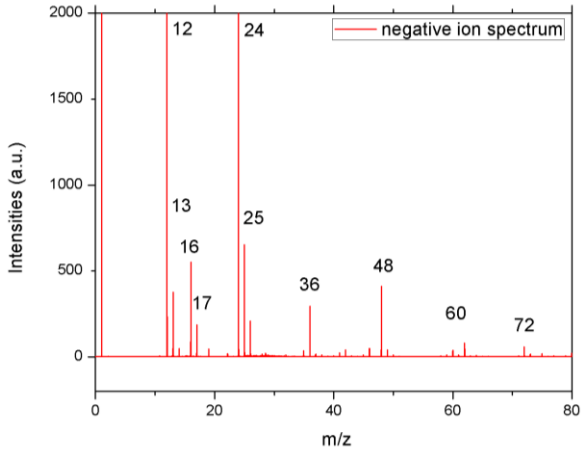

Table S1. List of negative fragment ions			
m/z	fragment	m/z	fragment
12	C^-	25	C_2H^-
13	CH^-	36	C_3^-
16	O^-	48	C_4^-
17	OH^-	60	C_5^-
24	C_2^-	72	C_6^-

Figure S6. The TOF-SIMS negative ion spectrum of the HOPG after Ar_{2500}^+ ion sputtering. C_xH_y fragments with low content of hydrogen were observed. It's clearly shown that C_xH_y fragmentation patterns with a low hydrogen content is the signature characteristic of graphitic materials.

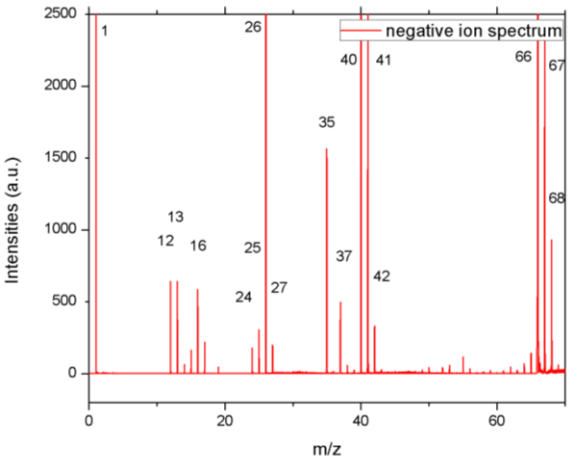

Table S3. List of negative fragment ions			
m/z	fragment	m/z	fragment
1	H^-	35	Cl^-
12	C^-	37	Cl^-
13	CH^-	40	CN_2^-
16	O^-	41	CN_2H^-
24	C_2^-	42	$CN_2H_2^-$
25	C_2H^-	66	$C_2N_3^-$
26	CN^-	67	$C_2N_3H^-$
27	CNH^-	68	$C_2N_3H_2^-$

Figure S7. The TOF-SIMS negative ion spectrum of the melamine standard after Ar_{2500}^+ ion sputtering. $C_xN_yH_z$ fragments with high content of hydrogen were observed.

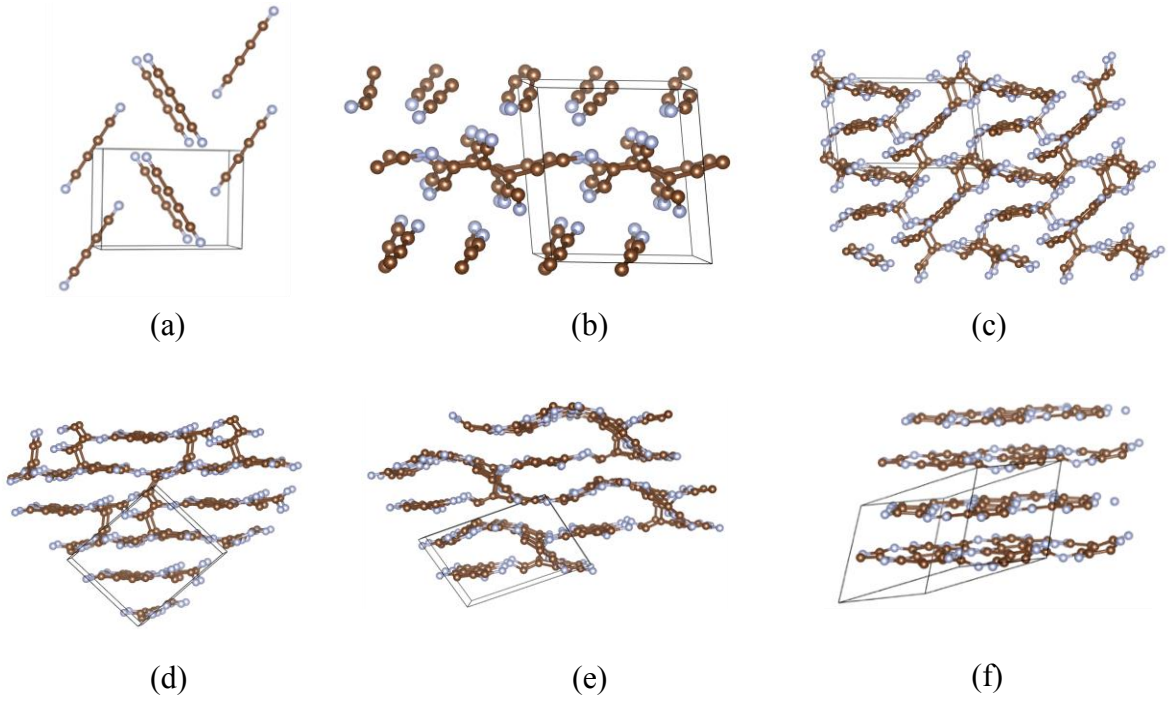

Figure S8. Transition from the $P2_1/c$ molecular structure to the amorphous layered structure based on metadynamics simulations. Several different abrupt transitions can easily be identified during the metadynamics run. In the first transition (b), the linear C_4N_2 molecules in the simulation cell disappeared and chair-like chains were created. At metastep 47, the intermediate state (b) transitions to a lower enthalpy structure (c), in which the C-N belts are connected by sp^3 bonded carbon atoms, forming a three-dimensional structure. The transition to (d), starting at metadynamics step 100, leads to a quasi-two-dimensional structure. The graphite-like sheets are linked by carbon-carbon bonds in the structure (d). After overcoming a high barrier at metastep 212, the sheets start to bend drastically forming a curved wave-like structure (e), in which the C-N six-member rings connect the neighboring 'wave'. The equilibrium structure (f) was finally created after metastep 500 (200 ps). This structure has two-dimensional character.

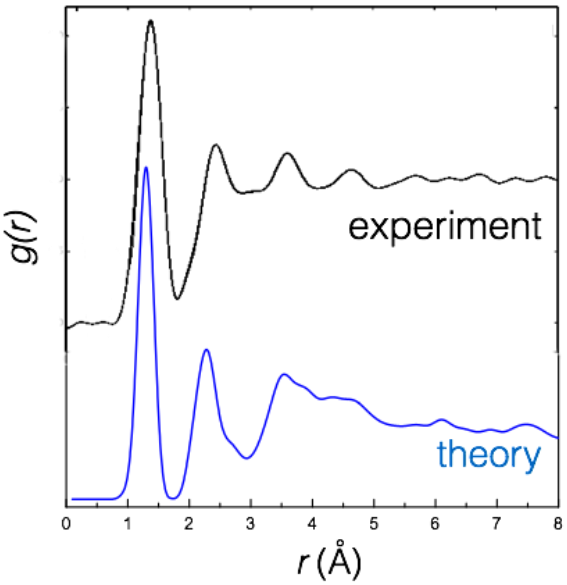

Figure S9. Experimental $g(r)$ compared with calculated $g(r)$ from metadynamics calculations (structure (f) in Fig. S8). This calculated radial distribution function is similar, but distinct from the one obtained from molecular dynamics simulations (shown in the main text).

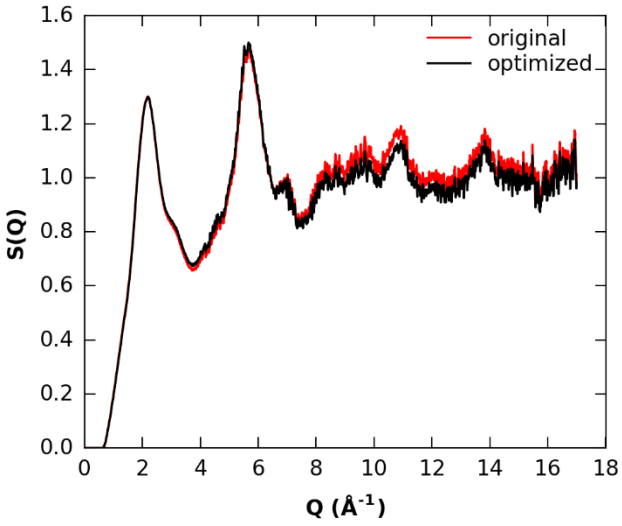

Figure S10. Comparison of original and optimized structure factors $S(Q)$ of the decompressed recovered sample. Optimization was performed by Kaplow-type correction with 3 iterations.

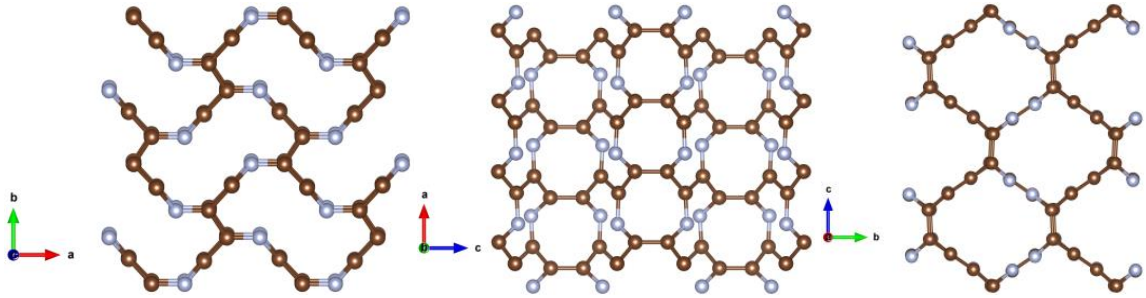

Figure S11. Predicted metastable 3D C_4N_2 structure by evolutionary metadynamics in USPEX in [100], [010] [001] directions

_symmetry_space_group_name_	'P212121'
_symmetry_Int_Tables_number	19
_symmetry_cell_setting	orthorhombic
_cell_length_a	5.8499
_cell_length_b	5.6832
_cell_length_c	6.9881
_cell_angle_alpha	90.0000
_cell_angle_beta	90.0000
_cell_angle_gamma	90.0000

C1	C	0.80925	0.39727	0.70225
C2	C	0.84215	0.75227	0.90245
C3	C	0.34168	0.73625	0.90503
C4	C	0.30995	0.08255	0.69353
N5	N	0.97217	0.89737	0.78822
N6	N	0.52880	0.08065	0.69955

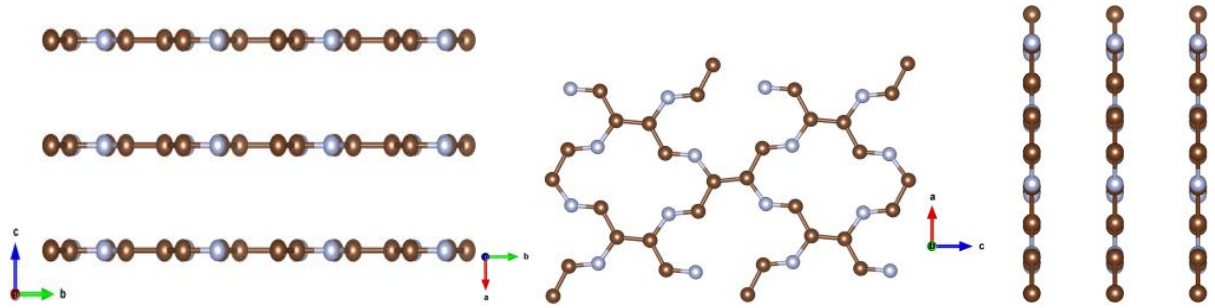

Figure S12. Predicted metastable 2D C_4N_2 structure by evolutionary metadynamics in USPEX in [100], [010] [001] directions

_symmetry_space_group_name_	'PBAM'			
_symmetry_Int_Tables_number	55			
_symmetry_cell_setting	orthorhombic			
_cell_length_a	4.8751			
_cell_length_b	8.1667			
_cell_length_c	2.8702			
_cell_angle_alpha	90.0000			
_cell_angle_beta	90.0000			
_cell_angle_gamma	90.0000			
C1	C	0.51416	0.58491	0.00000
C2	C	0.76855	0.66644	0.00000
N3	N	0.78991	0.81801	0.00000

References

1. Hannan, R. B.; Collin, R. L., The crystal structure of dicyanoacetylene. Acta Crystallographica 1953, 6 (4), 350-352.
2. Khanna, R. K.; Perera-Jarmer, M. A.; Ospina, M. J., Vibrational infrared and Raman spectra of dicyanoacetylene. Spectrochimica Acta Part A: Molecular Spectroscopy 1987, 43 (3), 421-425.
3. Brown, K. W.; Nibler, J. W.; Hedberg, K.; Hedberg, L., Structure of dicyanoacetylene by electron diffraction and coherent rotational Raman spectroscopy. The Journal of Physical Chemistry 1989, 93 (15), 5679-5684.